

PAPER • OPEN ACCESS

Energy harvesting from the vibrations of a passing train: effect of speed variability

To cite this article: V G Cleante *et al* 2016 *J. Phys.: Conf. Ser.* **744** 012080

View the [article online](#) for updates and enhancements.

Related content

- [Characterization of a variable reluctance harvester](#)
M Kroener, N Moll, S K T Ravindran *et al.*
- [Variable reluctance harvester for applications in railroad monitoring](#)
M Kroener, S K T Ravindran and P Woias
- [Modeling on energy harvesting from a railway system using piezoelectric transducers](#)
Jianjun Wang, Zhifei Shi, Hongjun Xiang *et al.*



IOP | ebooks™

Bringing you innovative digital publishing with leading voices to create your essential collection of books in STEM research.

Start exploring the collection - download the first chapter of every title for free.

Energy harvesting from the vibrations of a passing train: effect of speed variability

V G Cleante¹, M J Brennan¹, G Gatti² and D J Thompson³

¹Departamento de Engenharia Mecânica, UNESP, Ilha Solteira, 15385-000, Sao Paulo, Brazil.

²Department of Mechanical Energy and Management Engineering, University of Calabria, Arcavacata di Rende, Italy.

³Institute of Sound and Vibration Research, University of Southampton, Southampton, United Kingdom.

E-mail: vinicius_cleante@hotmail.com

Abstract. This paper builds on a previous study which investigated the amount of energy that could be harvested from the vibration induced by a passing train using a trackside energy harvester. In that study, the optimum parameters of the device were determined for a train passing at a particular speed. However, the effect of the train speed variability on the amount of energy harvested was not explored. In this paper a study is thus undertaken to determine this effect using experimental data from train passages at a site in the UK. Furthermore, a model is developed to investigate the optimum design parameters of the energy harvester when trains pass by at slightly different speeds. This is then validated using the experimental data. It is found that, provided the variability in the train speed is less than about 1% from the nominal speed, then a harvester tuned so that its natural frequency matches one of the trainload dominant frequencies at the line speed is a reasonable design condition.

1. Introduction

Many researchers have investigated the scavenging of energy from environmental vibrations for many years. Recently, the demand for sustainable devices has also increased, mainly to supply energy from devices embedded in environments with difficult access [1–3]. At the heart of many devices is a linear single-degree-of-freedom mass-spring-damper system, which is used to amplify vibration at a specific frequency. To achieve this, the oscillator is generally tuned so that its natural frequency is equal to the excitation frequency, and the damping is light [4].

Using classical models, researchers have conducted investigations based on harmonic base excitation for an unlimited time [5–8]. In such cases transient vibration is generally not considered. However, for applications such as a pacemaker [9], human motion [10], or railway vibration [11], where the source of vibration may only be present for a short period of time, transient vibration has to be considered.

Nowadays the vibration generated by a train is seen as potential energy source to power wireless sensors for structural health monitoring or temperature monitoring purposes, for example. An investigation using a piezoelectric transducer attached to the bottom of the rail to scavenge energy from vibration induced by loaded and unloaded freight trains was presented in [12]. An energy harvesting device was designed and embedded into a sleeper to convert the vertical vibration induced



by a passing train into a rotational motion and then into electrical energy in [13]. A numerical investigation about the potential to harvest energy from trackside vibration induced by high speed train in the UK was presented in [11, 14],

The aim of this paper is to develop further the work reported in [11], by investigating the effects of the variability of speed of the passing trains. This is achieved by developing a simple model of a passing train which is validated with some experimental measurements from a UK site.

2. Rail vibration due the passage of a train

The sleeper vibration presented here was measured at Steventon in Southern England from passing Inter-city 125 trains [15]. The structure of a rail track is shown in Fig. 1(a). The rail is fastened by clips to a concrete sleeper, which is supported by ballast and subgrade. The surrounding soil consists of deep layers of clay, which at the time of the measurement, was saturated [16]. The parameters of the rail structure at the Steventon site are given in Table 1. The model of the track structure is discussed later.

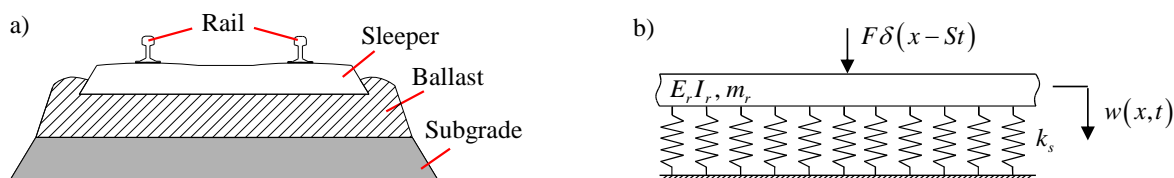


Figure 1 (a) example of the rail track structure; and (b) A simplified model of the track structure consisting of an Euler-Bernoulli infinite beam on a Winkler foundation subject to a concentrated moving load.

Table 1. Parameters of the rail structures at Steventon site (values for two rails) [16].

Parameters		Values
Rail	Bending stiffness	$1.26 \times 10^7 \text{ Nm}^2$
Rail pad	Stiffness	$2.10 \times 10^8 \text{ N/m}$
Ballast	Stiffness	$1.89 \times 10^8 \text{ N/m}$
Sleeper	Sleeper spacing	0.6 m

2.1. Vibration Measurements

The experimental data used here was obtained by Triepaischajonsak [15]. The train was an Inter-city 125 consisting of two power cars, one in each end, with eight passenger carriages in between. Each carriage is supported by four wheelsets contained in two bogies. The relevant train parameters are given in Table 2. The vibration induced by four trains, passing at speeds of 162, 180, 195 and 200 km/h, was measured on a railway sleeper using an accelerometer with a sampling frequency of 1 kHz. The corresponding acceleration time histories are presented in figures 2(a,c,e,g), respectively. The corresponding power spectral densities (PSD) of the acceleration measurements are shown in figure 2(b,d,f,h), respectively, in the frequency range 0-25 Hz. At the top of the PSD plots there is another axis which represents the frequency normalized by the ratio between the speed and length of the passenger carriage (23 m). It can be seen that the dominant peaks occur at integer multiples of the ratio between the speed and the length of the train carriage, which are called trainload dominant frequencies [17]. It can also be seen that with an increase (decrease) of the train speed, the dominant frequencies shift to higher (lower) frequencies. As the amplitude of the acceleration spectrum is proportional to the amplitude of the displacement multiplied by the square of the frequency, the acceleration amplitude changes with the train speed. In addition, the maximum acceleration induced by an Inter-city 125 at Steventon occurs at the 7th harmonic of the fundamental trainload frequency.

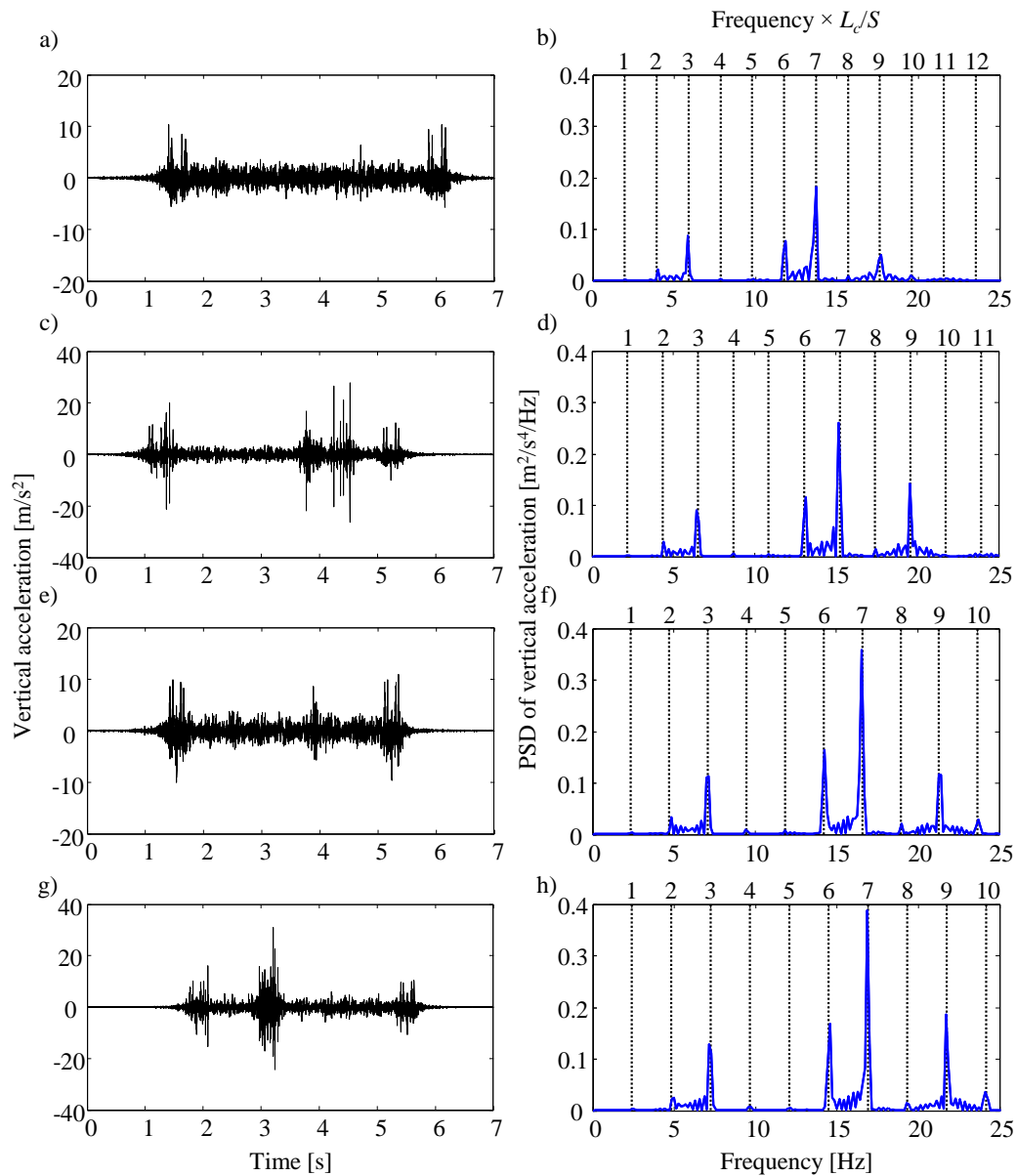


Figure 2. Time-history and power spectral density (PSD) measurement of the vertical acceleration of a sleeper due the passage of an Inter-city 125 train at speed of (a; e) 162 km/h; (b; f) 180 km/h; (c; g) 195 km/h; and (d; h) 200 km/h. (a–d) time-history, (e–h) PSD. The upper axis of the PSD shows the frequency normalized by the ratio between the train speed and the carriage length.

Table 2. Inter-city 125 parameters [16].

Parameters	Values
Bogie centres [m]	16
Bogie wheelbase [m]	2.6
Vehicle length [m]	23
Axle load [kN]	108.3

2.2. A simple model of a passing train and the track structure

To conduct a study into the effects of the variability of the train speeds on energy harvesting, a model comprising the train and the track structure is required. This is developed in this section. Grassie et al.

[18] have shown that for excitation frequencies up to 100 Hz, a track resting on a simple elastic support is satisfactory for the analysis of track deflection due to the static moving load. Krylov and Ferguson [19], Sheng et al. [20] and Thompson [21] have presented an analytical model, assuming that the two rails are modelled as a single infinite Euler-Bernoulli beam, which makes it possible to calculate the deflection $w(x,t)$ of the track due to the moving load. Such a simplified model is shown in figure 1(b). A concentrated load for each wheelset is applied to the track structure which is modelled as an infinite Euler Bernoulli beam with bending stiffness $E_r I_r$ (E_r is the Young's modulus and I_r is the second moment of area), supported by a series combination of rail pad and the ballast stiffness - a Winkler foundation of stiffness k_s per unit length. The differential equation of motion for the track for a stationary load F acting on a beam is given by [21]

$$E_r I_r \frac{d^4 w(x,t)}{dx^4} + k_s w(x,t) = F \delta(x-St) \quad (1)$$

where δ is the delta function, S is the train speed and x is the axial coordinate.

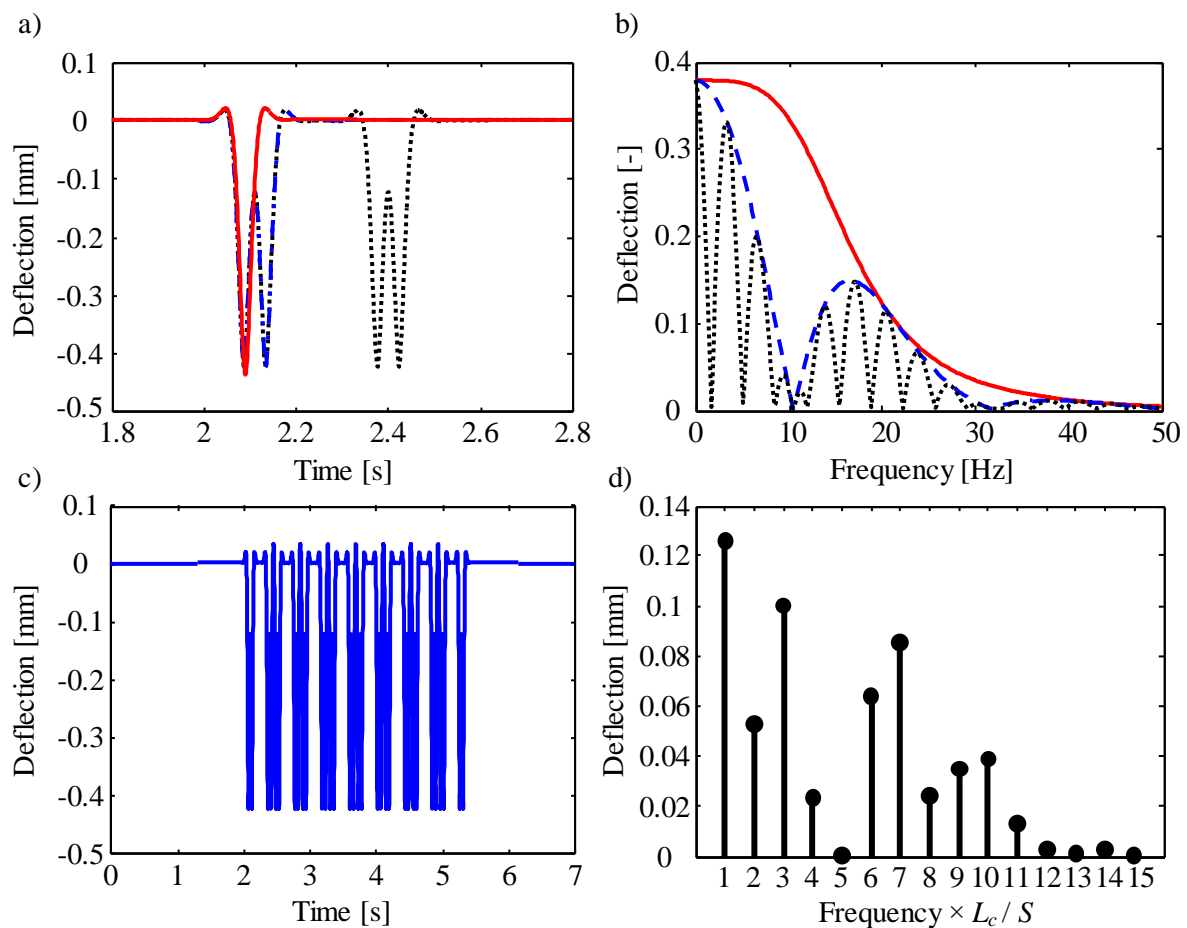


Figure 3. Vertical rail deflection due the passage of an Inter-city 125 HST at a speed of 200 km/h at Stevenston. (a) and (b) Time-history and spectrum, respectively, due the passage of one wheelset (— red solid line); one bogie (— · — blue dash-dot-dash line); and one passenger car (· · · black dotted line); and (c) and (d) Time-history and Fourier coefficients due the passage of 8 passenger cars.

The solution of equation (1) is [21]

$$w(x, t) = \frac{F\beta}{2k_s} e^{-\beta|x-St|} \left[\cos(\beta|x-St|) + \sin(\beta|x-St|) \right] \quad (2)$$

where $\beta = (k_s / (4E_r I_r))^{1/4}$ in which $k_s = (1/k_p + 1/k_b)^{-1} / L_s$ is the support stiffness, where k_p and k_b are the stiffness of the rail pad and the ballast, respectively, and L_s is the sleeper spacing.

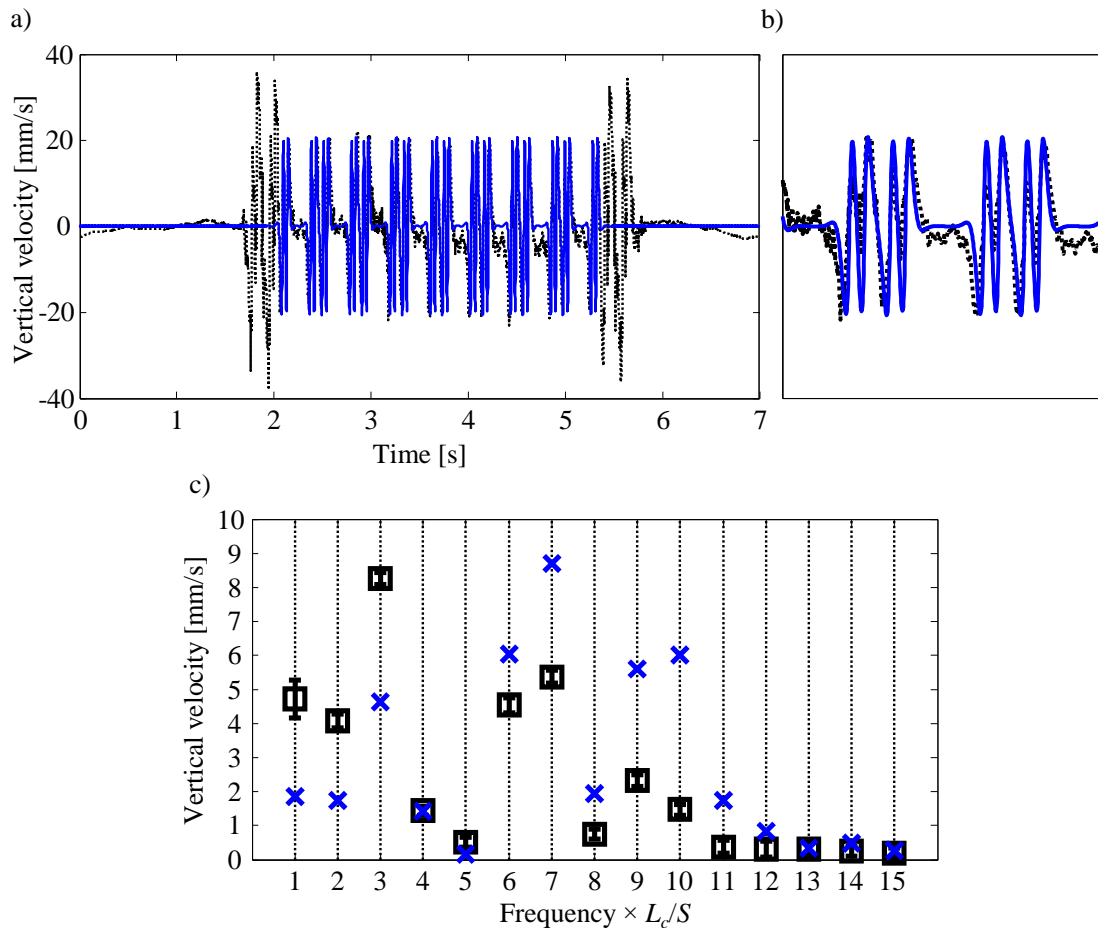


Figure 4. Comparison between vertical velocities measured at centre of a sleeper and the analytical model of rail deflection due the passage on an Inter-city 125 at a speed of 200 km/h at Steventon: (a) time-history, (b) zoom of a period of time from 3 to 4 seconds, (c) the Fourier coefficients. Black dotted line (\cdots) and black square (\square) correspond to measurement data. Black dash ($-$) is the standard deviation of the Fourier coefficients. Blue solid line ($-$) and blue cross (\times) correspond to the model.

Using equation (2) and the parameters for an Inter-city 125 train at a speed of 200 km/h and the parameter values given in Tables 1 and 2 some simulations are carried out. The displacement time-history of the track for the passage of one wheel, one bogie, and one passenger car are presented in figure 3a. The corresponding spectra are shown in figure 3b. From figure 3(a) it can be seen that each creates a small deflection of the rail over a very short period of time. This excitation mechanism causes a track deflection whose spectrum is similar to that from an impulse as shown in figure 3(b). It can be seen that the passage of a single wheelset at 200 km/h generates a spectrum with low frequency content, up to about 50 Hz. This spectrum is controlled by the train speed and by β . Thus, for a given rail stiffness, the stiffness of the support structure influences the frequency content. When more than one wheelset is considered, the effect of the bogie spacing or the carriage length affects the excitation

as shown in figure 3(a). The effect of this on the spectrum can be seen in figure 3(b), for a passage of a single bogie, and for the passage of a single train carriage. It can be observed that the envelope of the spectrum for a single train carriage is the deflection spectrum due the passage of a single bogie.

A similar simulation for 8 passenger carriages was carried out and the results are shown in figure 3(c) and (d). From figure 3(c) it can be seen that the time history is simply the superposition of 8 passenger carriages. In figure 3(d) the Fourier series coefficients is presented. The largest Fourier components correspond to the train load frequencies [17].

2.3. Comparison between the measured vibration and the model

The velocity of the rail calculated using the model from figure 1(b), assuming eight identical carriages (which neglects the power cars) is compared with experimental data. The results are shown in figure 4 for a train speed of 200 km/h. Given the simplicity of the model the results are considered to compare reasonably well in the time domain as can be seen in figures 4(a) and (b). The first 15 Fourier coefficients calculated from the passage of one carriage are plotted in figure 4(c). The agreement between the Fourier coefficients is not as good as the time histories, although the behaviour between the model and the actual train is qualitatively similar. This is thought to be due to the simplicity of the model and, probably, the choice for the parameters of the rail structure parameters, and is the subject of a current investigation. As the rail model is derived under the assumption of a continuous support, but in reality the rail is discretely supported by the sleepers, some physical behaviour of the rail may not be captured by the model and cause the discrepancy in frequency domain. However, from the point of view of the investigation into the variability of the train speed, it is suggested that the model is adequate to investigate energy harvesting is used in further analysis in later sections.

3. Energy Harvesting

3.1. Numerical investigation

The mechanical system of the energy harvester device considered here is a base-excited single-degree-of-freedom mass-spring-damper system, in which the base excitation is the acceleration of a sleeper, induced by a passing train. The equation of motion of such a system is given by

$$m\ddot{z}(t) + c\dot{z}(t) + kz(t) = -m\ddot{y}(t) \quad (3)$$

where the relative displacement is $z = x - y$, x is the motion of the oscillating mass and y is the motion of the base, m is the mass, c is the damping and k is the stiffness. The overdots denote differentiation with respect to time. For simplicity, here it is assumed that the total energy harvested E , is equal to the mechanical dissipated energy, so that

$$E = \int_0^{t_e} c \dot{z}^2 dt \quad (4)$$

Equation (3) is solved by numerical integration, using the vertical acceleration induced by an Inter-city 125 at a speed of 200 km/h given in figure 2(g) as a base input. It is then combined with equation (4) to determine the energy harvested during the passage of a train. Only the time period from 1.7 to 5.7 seconds, where the passing train induces forced vibration of the energy harvester is considered. Simulations have already been conducted to investigate the optimum parameters of the harvester to such an excitation [11], and the results of this study are presented here. The mass of the harvester is set to 1 kg and the natural frequency varied from 0.1 up to 35 Hz with an increment of 0.1429 Hz. Also the optimum damping ratio for each natural frequency is determined from a range of $1 \times 10^{-4} < \zeta < 5 \times 10^{-2}$ with an increment of 1×10^{-4} . The results from the numerical study are shown in figure 5 as the blue solid line. Figure 5(a) shows the maximum harvested energy for each natural frequency, figure 5(b) shows the optimum damping ratio necessary for the oscillator achieve its best performance, and figure 5(c) shows the maximum relative displacement amplitude of the oscillating mass. From figure 5(a) it can be seen that the frequencies at which the greatest amount of energy is harvested coincides

with the dominant trainload frequencies shown in figure 2(h). The harvester scavenges the maximum energy when the acceleration is maximum, corresponding to a frequency of 16.86 Hz, which is the 7th harmonic of the fundamental trainload frequency. For the natural frequencies where the oscillator harvests more energy, it can be seen that the oscillator requires very light damping. This is because it is better for the oscillator to have large relative motion, which can be seen in figure 5(c). From this numerical investigation it can be seen that the energy harvester should have a natural frequency of 16.86 Hz and a damping ratio of 0.0044. This results in 0.27 J of energy harvested from one train passage for 1 kg of mass with a relative displacement of about 5 mm.

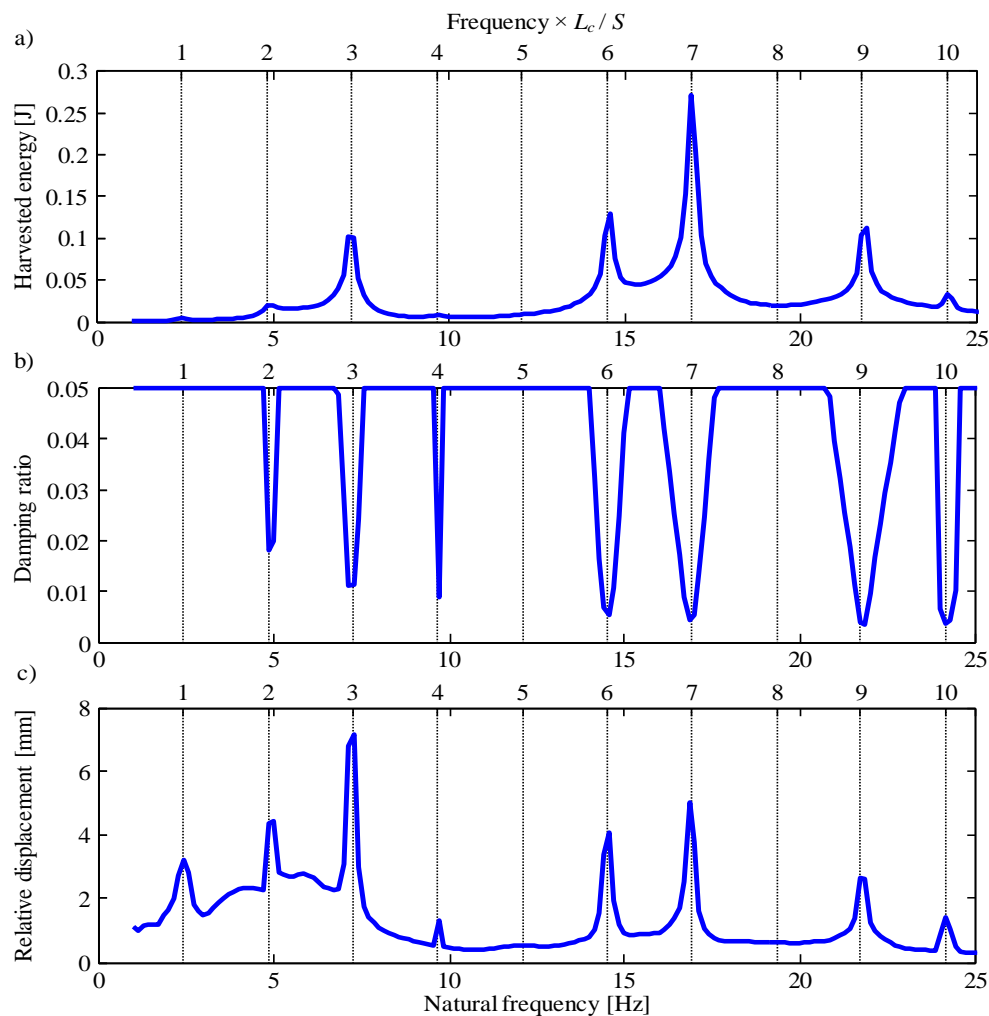


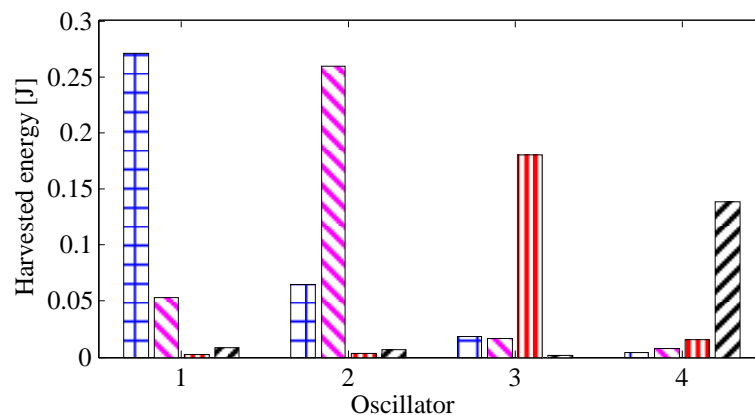
Figure 5. Result of the numerical analysis for an energy harvester with different natural frequency due the passage of an Inter-city 125 at a speed of 200 km/h: (a) Harvested energy; (b) Optimal damping ratio; and (c) Relative displacement.

To determine the sensitivity of the energy harvester to different train speeds, the harvesters were optimised for the four train time histories shown in figure 2, i.e., for trains operating at 162, 180, 195 and 200 km/h. The optimised conditions are given in Table 3.

The amount of energy harvested for each of the four harvesters as each train passes at the four different speeds is shown in figure 6. It can be seen that there is only a good performance for the harvester that is optimised for the particular train speed. For the other situations, the performance of the oscillator degrades drastically: even for the harvester intended for 200 km/h, less than 20% of the energy is harvested at 195 km/h.

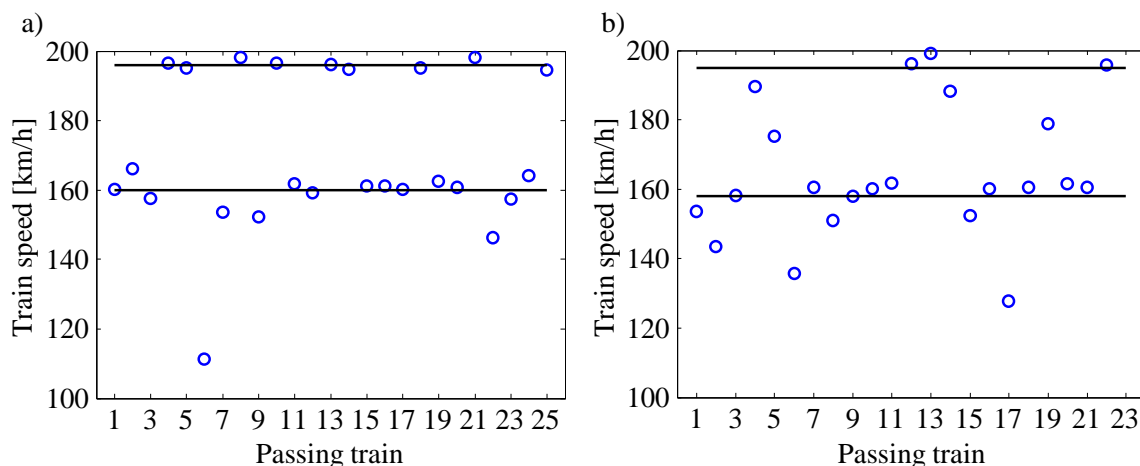
Table 3. Optimised energy harvester device parameter due to vibration induced by four Inter-city 125 trains passing at Steventon site.

Oscillator parameter	Train speed [km/h]			
	162	180	195	200
Natural frequency [Hz]	13.72	15.14	16.57	16.86
Harvested energy [J]	0.14	0.18	0.26	0.27
Damping ratio	0.0045	0.0046	0.0043	0.0044
Relative displacement [mm]	4.52	4.54	5.05	5.02

**Figure 6.** Energy harvested from harvesters with optimum parameters for a single passing train. Harvesters 1, 2, 3 and 4 are optimised for train speeds of 200, 195, 180 and 162 km/h respectively. Train speeds: 200 km/h, 195 km/h, 180 km/h, and 162 km/h.

4. Effects of different train speeds

In a railway environment, the speed of a train is restricted due to the route, the type of train and operational considerations. Although they operate at high speeds, this does not mean that the vehicle speed is constant throughout their journey, and it is not the same for all passing trains. The train speeds of passing trains were measured over two days at Steventon, where the train speed is limited to 200 km/h. The results are shown in figure 7, where it is clear that the variability of the train speeds at this site is, in general, quite high.

**Figure 7.** Speed of Inter-city 125 trains at Steventon measured during two days. (a) Day 1, (b) Day 2. (○) blue circle is the train speed; and (—) black solid line is the average.

From figure 7(a), it can be seen that there are two clusters, the average speeds of which are 160 and 196 km/h. The same is seen to be true in figure 7(b) where the average speeds are 158 and 195 km/h (only the highest five measurement speeds were considered for the upper average), but the scatter is much greater in this case. The reason why there are two average speeds is because there is a railway station close to the measurement site, and some trains stop at this station and others do not.

Of interest is the effect that the train speed variability has on the energy harvested from a device optimised for a particular speed. To investigate this, the models of the harvester and the track are used to conduct simulations on harvesters optimised for train speeds from 190 to 200 km/h with an increment of 1 km/h. The damping ratio is optimised to the combined energies due to the passage of eleven trains. The natural frequency of each oscillator is set to the 7th harmonic of the fundamental trainload frequency for each train. The energy harvested by each oscillator is shown in figure 8 and the sum of energy harvested by each oscillator, along with the optimised damping ratios is shown in Table 4.

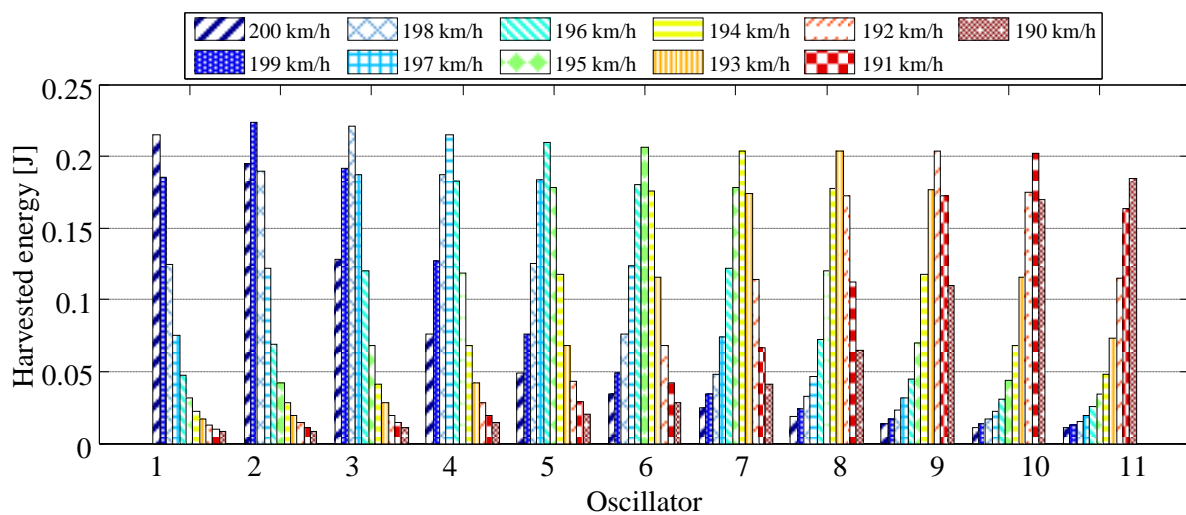


Figure 8. Energy harvested by a single oscillator from vibrations induced by a passing train with a range of speed of 190 to 200 km/h.

Table 4. Optimum parameters and total energy harvested from a single oscillator for a range of passing train speed from 190 to 200 km/h.

Oscillator	Frequency [Hz]	Damping ratio (10^{-3})	Sum of energy harvested [J]
1	16.90	7.590	0.748
2	16.82	6.495	0.922
3	16.74	6.583	1.030
4	16.65	6.969	1.081
5	16.57	7.276	1.100
6	16.48	7.418	1.099
7	16.40	7.430	1.081
8	16.31	7.277	1.043
9	16.23	6.984	0.980
10	16.14	6.972	0.870
11	16.06	8.556	0.702

The results in figure 8 clearly show that the optimal operational condition for an energy harvester is when it is operating at resonance. However, for passing trains, which excite frequencies close to the natural frequency of the energy harvester, the performance of the oscillator deteriorates slightly.

Moreover if there is a difference of 2 km/h or less in target train speed, the energy harvesters have a reasonable performance. From Table 4 is seen that the damping ratio, different from the optimized oscillator to a single passing train ($\zeta = 0.004547$), is slightly higher when there is more than one passing train inducing vibration. This increase in damping leads to a detrimental effect on the performance at resonance, but it has a beneficial effect on the harvester performance when it not at resonance. From the sleeper vibration induced by passing trains with a range of speed from 190 to 200 km/h, oscillator 5 has the best performance. It has a natural frequency of 16.65 Hz and a damping ratio of 0.007418. This oscillator is able to harvest a total of 1.1 J after the passage of eleven high speed trains.

5. Conclusions

This paper has investigated how much mechanical energy can potentially be harvested from the vertical vibration of a sleeper induced by trains passing at different speeds. To achieve this, a model of a track structure was combined with a model of an energy harvester. The models have been validated with experimental data from a site in the UK. It has been shown that the optimum operational condition for a linear energy harvester is when its natural frequency is tuned to the trainload dominant frequency with the largest acceleration amplitude. Further investigation has shown that when a single linear energy harvester is subject to vibration induced by passing trains at different speeds, the mechanical system presents a significant performance only for passing trains with a difference of 1% or less from the target train speed. For this specific case studied, for a range of trains at speeds from 190 to 200 km/h, the total energy that could be potentially harvested is about 1.1 J/kg, at a frequency of 16.65 Hz, which correspond to a passing train at speed of 196 km/h, with a damping ratio of 0.007276.

References

- [1] Danioni A G E, Marchesi M, Nucita V and Dallago V 2011 A self-powered electronic interface for electromagnetic energy harvester *Power Elec., IEEE transaction on* **26** pp 3174-3182
- [2] Lu X *et al* 2015 Performance analysis of simultaneous wireless information and power transfer with ambient RF energy harvester *ArXiv e-print*
- [3] Wischke M, Mansur M, Kroner M and Woias P 2011 Vibration harvesting in traffic tunnels to power wireless sensor nodes *S. M. and Struc.* **20** 085014
- [4] Stephen N G 2006 On energy harvesting from ambient vibration *J. of Sound and Vib.* **293** pp 3174-3182
- [5] Cassidy I L, Scruggs J T, Behrens S and Gavin H P 2011 Design and experimental characterization of an electromagnetic transducer for large-scale vibratory energy harvesting applications *J. of Int. Mat. Sys. and Struc.* **22** pp 2009-2024
- [6] Guyomar D, Jayet Y, Petit L, Lefeuvre E, Richard C and Lallart M 2007 Synchronized switch harvesting applied to selfpowered smart systems: Piezoactive microgenerators for autonomous wireless transmitters *Sen. and Actuator A: Phys.* **138** pp 151-160
- [7] Serre C, Pérez-Rodríguez A, Fondevilla N Martincic E, Morante J R, Montserrat J and Esteve J 2009 Linear and non-linear behaviour of mechanical resonators for optimized inertial electromagnetic microgenerators *Microsys. Technol.* **15** pp 1217-1223
- [8] Stephen N G 2006 On the maximum power transfer theorem within electromechanical systems *Proc. Inst. Mechan. Engin.* **220** pp 1261-1267
- [9] Karami M A and Inman D J Powering pacemakers from heartbeat vibration using linear and nonlinear energy harvesters *Appl. Phys. Letters* **147** pp 248-253
- [10] Saha C R, O'Donnell T, Wang N and McCloskey P 2008 Electromagnetic generator for harvesting energy from human motion *Sens. and Actuator A: Phys.* **147** pp 248-253
- [11] Gatti G, Brennan M J, Tehrani M G and Thompson D J 2016 Harvesting energy from the vibration of a passing train using a single-degree-of-freedom oscillator *Mech. Sys. and Sig. Proc.* **66-67** pp 785-792

- [12] Nelson C A, Platt S R, Albrecht D, Kamarajugadda V and Fateh M 2008 Power harvesting for railraoad track health monitoring using piezoelectric and inductive devies *Proc. Act. and Passive Smart Struc. and Integ. Sys.* **6928** 69280R
- [13] Hansen S E, Poughodrat A, Nelson C A and Fateh M 2010 On-track testing of a power harvesting device for railroad track health monitoring *Proc. Health Monitor. Struc. and Biol. Sys* **7650** 76500Y
- [14] Tehrani M G, Gatti G, Brennan M J and Thompson D J 2013 Energy harvesting from train vibration *11th Int. Conf. on Vibr. Prob. (ICOVP 2013)* (Lisbon: Portugal) pp 9-12
- [15] Triepaischajonsak N 2012 The influence of various excitation mechanisms on ground vibration from trains *University of Southampton*
- [16] Triepaischajonsak N, Thompson D J, Jones C J C, Ryue J and Pries J A 2011 Ground vibration from trains: Expertimental parameter characterization and validation of a numerical model *Proc. Of the Inst. Of Mech. Eng, Part F: J. of Rail and Rapid Transit* **225** pp140-153
- [17] Ju S –H, Lin H –T and Huang J Y 2009 Dominant frequencies of train-induced vibrations *J. of S. and Vib.* **319** pp 247-259
- [18] Grassie S L, Gregory R W, Harrison D and Johnson K L 1982 The dynamic response of railway track to high frequency vertical excitation *J. of Mech. Eng. Sci.* **24** pp 77-90
- [19] Krylov V and Ferguson C 1994 Calculation of low-frequency ground vibrations from railway trains *Appl. Accous.* **42** pp 199-213
- [20] Sheng X, Jones C J C and Petyt M 1999 Ground vibration generated by a load moving along a railway track *J. of Sou. And Vib.* **228** pp 129-156
- [21] Thompson D J 2008 Railway noise and vibration: mechanical modelling and means of control *Elsevier*